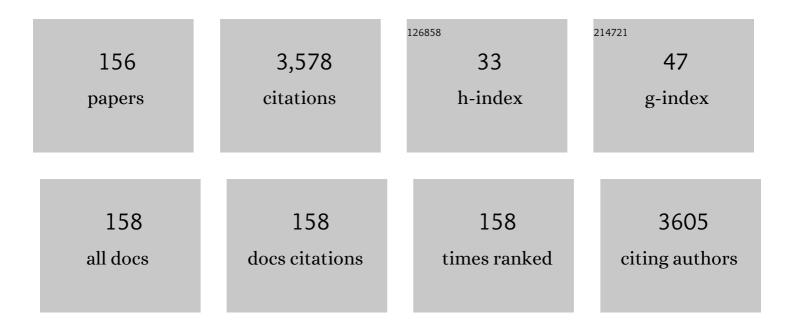
List of Publications by Year in descending order

Source: https://exaly.com/author-pdf/6201397/publications.pdf Version: 2024-02-01



ΙΠΙΓΕΤΤΑ ΡΑΠ

#	Article	IF	CITATIONS
1	Raman Spectroscopy in Skeletal Tissue Disorders and Tissue Engineering: Present and Prospective. Tissue Engineering - Part B: Reviews, 2022, 28, 949-965.	2.5	5
2	A review on current research status of the surface modification of Zn-based biodegradable metals. Bioactive Materials, 2022, 7, 192-216.	8.6	72
3	Factors influencing the drug release from calcium phosphate cements. Bioactive Materials, 2022, 7, 341-363.	8.6	52
4	Influence of Synthesis Conditions on Gadolinium-Substituted Tricalcium Phosphate Ceramics and Its Physicochemical, Biological, and Antibacterial Properties. Nanomaterials, 2022, 12, 852.	1.9	12
5	DEVELOPMENT OF NITROFURAN DERIVATIVE: COMPOSITION AND TECHNOLOGY OF EFFERVESCENT TABLETS WITH SOLID DISPERSIONS. Farmatsiya I Farmakologiya, 2022, 10, 55-68.	0.2	1
6	Pathway to tailor the phase composition, microstructure and mechanical properties of pulsed laser deposited cobalt-substituted calcium phosphate coatings on titanium. Surface and Coatings Technology, 2022, 437, 128275.	2.2	1
7	Antimicrobial properties of co-doped tricalcium phosphates Ca3-2(MËŠMËŠËŠ) (PO4)2 (M = Zn2+, Cu2+, Mn2+)	TjEŢQq1 2.3	1 0,784314 12
8	Strontium Substituted Tricalcium Phosphate Bone Cement: Short and Longâ€Term Timeâ€Resolved Studies and In Vitro Properties. Advanced Materials Interfaces, 2022, 9, .	1.9	15
9	Mn-Containing Bioactive Glass-Ceramics: BMP-2-Mimetic Peptide Covalent Grafting Boosts Human-Osteoblast Proliferation and Mineral Deposition. Materials, 2022, 15, 4647.	1.3	9
10	Biocompatible composite films and fibers based on Poly(Vinyl alcohol) and powders of calcium salts. Smart Materials in Medicine, 2021, 2, 292-301.	3.7	3
11	Adipogenic, chondrogenic, osteogenic, and antimicrobial features of glass ceramic material supplemented with manganese. Journal of Non-Crystalline Solids, 2021, 559, 120709.	1.5	8
12	High-Fat Diet Impairs Mouse Median Eminence: A Study by Transmission and Scanning Electron Microscopy Coupled with Raman Spectroscopy. International Journal of Molecular Sciences, 2021, 22, 8049.	1.8	5
13	EFFECT OF SOLID DISPERSIONS ON THE SOLUBILITY OF METRONIDAZOLE. Farmatsiya I Farmakologiya, 2021, 9, 195-204.	0.2	3
14	Ionized jet deposition of antimicrobial and stem cell friendly silver-substituted tricalcium phosphate nanocoatings on titanium alloy. Bioactive Materials, 2021, 6, 2629-2642.	8.6	21
15	Resorbable Mg2+-Containing Phosphates for Bone Tissue Repair. Materials, 2021, 14, 4857.	1.3	30
16	Improved cytocompatibility and antibacterial properties of zinc-substituted brushite bone cement based on β-tricalcium phosphate. Journal of Materials Science: Materials in Medicine, 2021, 32, 99.	1.7	34
17	Antibacterial and cell-friendly copper-substituted tricalcium phosphate ceramics for biomedical implant applications. Materials Science and Engineering C, 2021, 129, 112410.	3.8	33
18	In vitro characterization of novel nanostructured collagen-hydroxyapatite composite scaffolds doped with magnesium with improved biodegradation rate for hard tissue regeneration. Bioactive Materials, 2021, 6, 3383-3395.	8.6	38

#	Article	IF	CITATIONS
19	Manganese-containing bioactive glass enhances osteogenic activity of TiO2 nanotube arrays. Applied Surface Science, 2021, 570, 151163.	3.1	10
20	Design of 3D Additively Manufactured Hybrid Structures for Cranioplasty. Materials, 2021, 14, 181.	1.3	26
21	Thermal crystallization of amorphous calcium phosphate combined with citrate and fluoride doping: a novel route to produce hydroxyapatite bioceramics. Journal of Materials Chemistry B, 2021, 9, 4832-4845.	2.9	18
22	Quality control methods in musculoskeletal tissue engineering: from imaging to biosensors. Bone Research, 2021, 9, 46.	5.4	10
23	Additives Imparting Antimicrobial Properties to Acrylic Bone Cements. Materials, 2021, 14, 7031.	1.3	12
24	Composite Polyvinylpyrrolidone–Sodium Alginate—Hydroxyapatite Hydrogel Films for Bone Repair and Wound Dressings Applications. Polymers, 2021, 13, 3989.	2.0	14
25	Modification of PMMA Cements for Cranioplasty with Bioactive Glass and Copper Doped Tricalcium Phosphate Particles. Polymers, 2020, 12, 37.	2.0	19
26	In Vitro Properties of Manganese-Substituted Tricalcium Phosphate Coatings for Titanium Biomedical Implants Deposited by Arc Plasma. Materials, 2020, 13, 4411.	1.3	24
27	Comparability of Raman Spectroscopic Configurations: A Large Scale Cross-Laboratory Study. Analytical Chemistry, 2020, 92, 15745-15756.	3.2	46
28	Borate and Silicate Bioactive Glass Coatings Prepared by Nanosecond Pulsed Laser Deposition. Coatings, 2020, 10, 1105.	1.2	11
29	Novel Hybrid Composites Based on PVA/SeTiO2 Nanoparticles and Natural Hydroxyapatite for Orthopedic Applications: Correlations between Structural, Morphological and Biocompatibility Properties. Materials, 2020, 13, 2077.	1.3	32
30	Pulsed laser deposition temperature effects on strontium-substituted hydroxyapatite thin films for biomedical implants. Cell Biology and Toxicology, 2020, 36, 537-551.	2.4	18
31	Tricalcium phosphate cement supplemented with boron nitride nanotubes with enhanced biological properties. Materials Science and Engineering C, 2020, 114, 111044.	3.8	13
32	Characterization of Scardovia wiggsiae Biofilm by Original Scanning Electron Microscopy Protocol. Microorganisms, 2020, 8, 807.	1.6	31
33	Influence of oblique angle deposition on Cu-substituted hydroxyapatite nano-roughness and morphology. Surface and Coatings Technology, 2020, 394, 125883.	2.2	19
34	Iron Ionâ€Doped Tricalcium Phosphate Coatings Improve the Properties of Biodegradable Magnesium Alloys for Biomedical Implant Application. Advanced Materials Interfaces, 2020, 7, 2000531.	1.9	31
35	Colloidal forming of macroporous calcium pyrophosphate bioceramics in 3D-printed molds. Bioactive Materials, 2020, 5, 309-317.	8.6	11
36	Electrospun poly(<scp>d,l</scp> â€lactide)/gelatin/glass eramics tricomponent nanofibrous scaffold for bone tissue engineering. Journal of Biomedical Materials Research - Part A, 2020, 108, 1064-1076.	2.1	24

#	Article	IF	CITATIONS
37	Controlling the Degradation Rate of Biodegradable Mg–Zn-Mn Alloys for Orthopedic Applications by Electrophoretic Deposition of Hydroxyapatite Coating. Materials, 2020, 13, 263.	1.3	36
38	Biocompatibility of biphasic α,β-tricalcium phosphate ceramics in vitro. Bioactive Materials, 2020, 5, 423-427.	8.6	30
39	Properties and in vitro assessment of ZrO2-based coatings obtained by atmospheric plasma jet spraying on biodegradable Mg-Ca and Mg-Ca-Zr alloys. Ceramics International, 2020, 46, 15897-15906.	2.3	36
40	Modification of titanium surface via Ag-, Sr- and Si-containing micro-arc calcium phosphate coating. Bioactive Materials, 2019, 4, 224-235.	8.6	61
41	Sic Parvis Magna: Manganese-Substituted Tricalcium Phosphate and Its Biophysical Properties. ACS Biomaterials Science and Engineering, 2019, 5, 6632-6644.	2.6	37
42	Flower-like aluminium nitride nanostructures deposited by rf magnetron sputtering on superhard rhodium boride films. Applied Physics A: Materials Science and Processing, 2019, 125, 1.	1.1	2
43	Glancing Angle Deposition of Zn-Doped Calcium Phosphate Coatings by RF Magnetron Sputtering. Coatings, 2019, 9, 220.	1.2	25
44	Raman Spectroscopy as a Diagnostic Tool Applied for Tissue Pathologies to Support Histological Analysis. Proceedings (mdpi), 2019, 27, 6.	0.2	0
45	Femtosecond Pulsed Laser Deposition of Chromium Diboride-Rich Thin Films. Coatings, 2019, 9, 777.	1.2	4
46	Cu-Releasing Bioactive Glass Coatings and Their in Vitro Properties. ACS Applied Materials & Interfaces, 2019, 11, 5812-5820.	4.0	49
47	Laser synthesis of iron nanoparticle for Fe doped hydroxyapatite coatings. Materials Chemistry and Physics, 2019, 225, 365-370.	2.0	19
48	Raman spectroscopy discriminates malignant follicular lymphoma from benign follicular hyperplasia and from tumour metastasis. Talanta, 2019, 194, 763-770.	2.9	13
49	Gold is for the mistress, silver for the maid: Enhanced mechanical properties, osteoinduction and antibacterial activity due to iron doping of tricalcium phosphate bone cements. Materials Science and Engineering C, 2019, 94, 798-810.	3.8	34
50	Pulsed laser deposited bioactive RKKP-Mn glass-ceramic coatings on titanium. Surface and Coatings Technology, 2019, 357, 122-128.	2.2	13
51	Raman Spectroscopy Applied to Parathyroid Tissues: A New Diagnostic Tool to Discriminate Normal Tissue from Adenoma. Analytical Chemistry, 2018, 90, 847-854.	3.2	30
52	Deposition of polycrystalline zinc substituted hydroxyapatite coatings with a columnar structure by RF magnetron sputtering: role of in-situ substrate heating. Journal of Physics: Conference Series, 2018, 1115, 032077.	0.3	13
53	Hydroxyapatite coatings on Mg-Ca alloy prepared by Pulsed Laser Deposition: Properties and corrosion resistance in Simulated Body Fluid. Ceramics International, 2018, 44, 16678-16687.	2.3	40
54	The Bone Building Blues: Self-hardening copper-doped calcium phosphate cement and its in vitro assessment against mammalian cells and bacteria. Materials Science and Engineering C, 2017, 79, 270-279.	3.8	55

#	Article	IF	CITATIONS
55	Pulsed laser-deposited composite carbon–glass–ceramic films with improved hardness. Journal of Materials Science, 2017, 52, 9140-9150.	1.7	8
56	Structural modification of titanium surface by octacalcium phosphate via Pulsed Laser Deposition and chemical treatment. Bioactive Materials, 2017, 2, 101-107.	8.6	17
57	Exploring challenges ahead of nanotechnology for biomedicine. Bioactive Materials, 2017, 2, 119-120.	8.6	3
58	Nonlinear oscillatory dynamics of the hardening of calcium phosphate bone cements. RSC Advances, 2017, 7, 40517-40532.	1.7	12
59	RF magnetron-sputtered coatings deposited from biphasic calcium phosphate targets for biomedical implant applications. Bioactive Materials, 2017, 2, 170-176.	8.6	32
60	Proof-of-concept Raman spectroscopy study aimed to differentiate thyroid follicular patterned lesions. Scientific Reports, 2017, 7, 14970.	1.6	20
61	THIN BIOACTIVE Zn-SUBSTITUTED HYDROXYAPATITE COATING DEPOSITED ON TI SUBSTRATE BY RADIOFREQUENCY SPUTTERING. High Temperature Material Processes, 2017, 21, 191-201.	0.2	1
62	Placenta Derived Mesenchymal Stem Cells Hosted on RKKP Glass-Ceramic: A Tissue Engineering Strategy for Bone Regenerative Medicine Applications. BioMed Research International, 2016, 2016, 1-11.	0.9	10
63	Bioactive Materials for Bone Tissue Engineering. BioMed Research International, 2016, 2016, 1-3.	0.9	39
64	Silver-Doped Calcium Phosphate Bone Cements with Antibacterial Properties. Journal of Functional Biomaterials, 2016, 7, 10.	1.8	36
65	A compact, coherent light source system architecture. Proceedings of SPIE, 2016, , .	0.8	0
66	Glass-ceramic coated Mg-Ca alloys for biomedical implant applications. Materials Science and Engineering C, 2016, 64, 362-369.	3.8	64
67	RBP1 bioactive glass-ceramic films obtained by Pulsed Laser Deposition. Materials Letters, 2016, 175, 195-198.	1.3	23
68	Zinc-releasing calcium phosphate cements for bone substitute materials. Ceramics International, 2016, 42, 17310-17316.	2.3	28
69	RAMAN spectroscopy imaging improves the diagnosis of papillary thyroid carcinoma. Scientific Reports, 2016, 6, 35117.	1.6	30
70	Pulsed laser ablation and deposition of niobium carbide. Applied Surface Science, 2016, 374, 112-116.	3.1	5
71	Two-Color Radiation Generated in a Seeded Free-Electron Laser with Two Electron Beams. Physical Review Letters, 2015, 115, 014801.	2.9	22
72	Novel approach to obtain composite poly-L-lactide based films blended with starch and calcium phosphates and their bioactive properties. Biomedical Physics and Engineering Express, 2015, 1, 045011.	0.6	9

#	Article	IF	CITATIONS
73	Bioactive, nanostructured <scp>S</scp> iâ€substituted hydroxyapatite coatings on titanium prepared by pulsed laser deposition. Journal of Biomedical Materials Research - Part B Applied Biomaterials, 2015, 103, 1621-1631.	1.6	62
74	Interdisciplinary approach to cell–biomaterial interactions: biocompatibility and cell friendly characteristics of RKKP glass–ceramic coatings on titanium. Biomedical Materials (Bristol), 2015, 10, 035005.	1.7	16
75	Pathway to a compact SASE FEL device. Nuclear Instruments and Methods in Physics Research, Section A: Accelerators, Spectrometers, Detectors and Associated Equipment, 2015, 798, 144-151.	0.7	3
76	Structural transformations in hydroxyapatite ceramics as a result of severe plastic deformation. Ceramics International, 2015, 41, 10526-10530.	2.3	3
77	Dual color x-rays from Thomson or Compton sources. , 2015, , .		1
78	Seeded FEL with two energy level electron beam distribution at SPARC_LAB. Proceedings of SPIE, 2015, , .	0.8	0
79	Fullerene-reduced graphene oxide composites obtained by ultrashort laser ablation of fullerite in water. Applied Surface Science, 2015, 336, 67-72.	3.1	9
80	Self-amplified spontaneous emission free electron laser devices and nonideal electron beam transport. Physical Review Special Topics: Accelerators and Beams, 2014, 17, .	1.8	3
81	Large-bandwidth two-color free-electron laser driven by a comb-like electron beam. New Journal of Physics, 2014, 16, 033018.	1.2	35
82	Mapping the transverse coherence of the self amplified spontaneous emission of a free-electron laser with the heterodyne speckle method. Optics Express, 2014, 22, 30013.	1.7	18
83	Dual color x rays from Thomson or Compton sources. Physical Review Special Topics: Accelerators and Beams, 2014, 17, .	1.8	17
84	IRIDE: Interdisciplinary research infrastructure based on dual electron linacs and lasers. Nuclear Instruments and Methods in Physics Research, Section A: Accelerators, Spectrometers, Detectors and Associated Equipment, 2014, 740, 138-146.	0.7	9
85	Fe-doped hydroxyapatite coatings for orthopedic and dental implant applications. Applied Surface Science, 2014, 307, 301-305.	3.1	46
86	SPARC_LAB present and future. Nuclear Instruments & Methods in Physics Research B, 2013, 309, 183-188.	0.6	124
87	Femtosecond pulsed laser ablation of molybdenum carbide: Nanoparticles and thin film characteristics. Applied Surface Science, 2013, 278, 321-324.	3.1	6
88	Two-phase zirconium boride thin film obtained by ultra-short pulsed laser ablation of a ZrB12 target. Applied Surface Science, 2013, 283, 715-721.	3.1	5
89	Nanostructured Si-substituted hydroxyapatite coatings for biomedical applications. Thin Solid Films, 2013, 543, 167-170.	0.8	37
90	Superradiant Cascade in a Seeded Free-Electron Laser. Physical Review Letters, 2013, 110, 044801.	2.9	46

#	Article	IF	CITATIONS
91	Observation of Time-Domain Modulation of Free-Electron-Laser Pulses by Multipeaked Electron-Energy Spectrum. Physical Review Letters, 2013, 111, 114802.	2.9	68
92	High-Order-Harmonic Generation and Superradiance in a Seeded Free-Electron Laser. Physical Review Letters, 2012, 108, 164801.	2.9	38
93	SASE FEL Storage Ring. IEEE Journal of Quantum Electronics, 2012, 48, 1259-1264.	1.0	6
94	Structural Study of Octacalcium Phosphate Bone Cement Conversion in Vitro. ACS Applied Materials & Interfaces, 2012, 4, 6202-6210.	4.0	22
95	Nanostructured molybdenum carbide thin films obtained by femtosecond pulsed laser deposition. Physica Status Solidi C: Current Topics in Solid State Physics, 2012, 9, 2370-2373.	0.8	5
96	Thin films deposited by femtosecond pulsed laser ablation of tungsten carbide. Applied Surface Science, 2012, 258, 9198-9201.	3.1	13
97	IR and X-ray time-resolved simultaneous experiments:Âan opportunity to investigate the dynamics of complex systems and non-equilibrium phenomena using third-generation synchrotron radiation sources. Journal of Synchrotron Radiation, 2012, 19, 892-904.	1.0	18
98	FEL SASE and wave undulators. Optics Communications, 2012, 285, 5341-5346.	1.0	9
99	Phase Development During Setting and Hardening of a Bone Cement Based on α-Tricalcium and Octacalcium Phosphates. Journal of Biomaterials Applications, 2012, 26, 1051-1068.	1.2	9
100	Time-domain measurement of a self-amplified spontaneous emission free-electron laser with an energy-chirped electron beam and undulator tapering. Applied Physics Letters, 2012, 101, 134102.	1.5	20
101	Bioactive glass–ceramic coatings prepared by pulsed laser deposition from RKKP targets (sol–gel vs) Tj ETQq	1 1 0.784 2.7	-314_rgBT /0
102	Single-phase bone cement based on dicalcium phosphate dihydrate powder and sodium silicate solution. Materials Letters, 2012, 73, 115-118.	1.3	19
103	Superhard Tungsten Tetraboride Films Prepared by Pulsed Laser Deposition Method. ACS Applied Materials & Interfaces, 2011, 3, 3738-3743.	4.0	50
104	Influence of Chitosan Glutamate on the in vivo Intranasal Absorption of Rokitamycin from Microspheres. Journal of Pharmaceutical Sciences, 2011, 100, 1488-1502.	1.6	51
105	Characterization of gaseous phase and nanoparticles produced in ultra-short pulsed laser ablation of transition metal borides. Applied Surface Science, 2011, 257, 5315-5318.	3.1	8
106	Diamond-like carbon thin films produced by femtosecond pulsed laser deposition of fullerite. Surface and Coatings Technology, 2011, 205, 3747-3753.	2.2	21
107	High-Gain Harmonic-Generation Free-Electron Laser Seeded by Harmonics Generated in Gas. Physical Review Letters, 2011, 107, 224801.	2.9	76
108	Self-amplified spontaneous emission for a single pass free-electron laser. Physical Review Special Topics: Accelerators and Beams, 2011, 14, .	1.8	60

#	Article	IF	CITATIONS
109	Self-Amplified Spontaneous Emission Free-Electron Laser with an Energy-Chirped Electron Beam and Undulator Tapering. Physical Review Letters, 2011, 106, 144801.	2.9	66
110	Elucidation of realâ€ŧime hardening mechanisms of two novel highâ€strength calcium phosphate bone cements. Journal of Biomedical Materials Research - Part B Applied Biomaterials, 2010, 93B, 74-83.	1.6	3
111	Real-time monitoring of the mechanism of poorly crystalline apatite cement conversion in the presence of chitosan, simulated body fluid and human blood. Dalton Transactions, 2010, 39, 11412.	1.6	18
112	Crystallization process of carbonate substituted hydroxyapatite nanoparticles in toothpastes upon physiological conditions: an in situ time-resolved X-ray diffraction study. Journal of Materials Science: Materials in Medicine, 2010, 21, 445-450.	1.7	18
113	Properties of pulsed laser deposited fluorinated hydroxyapatite films on titanium. Materials Research Bulletin, 2010, 45, 1304-1310.	2.7	25
114	In situ time-resolved X-ray diffraction study of octacalcium phosphate transformations under physiological conditions. Journal of Crystal Growth, 2010, 312, 2113-2116.	0.7	10
115	Deposition and characterisation of MoSi2 films. Thin Solid Films, 2010, 518, 2050-2055.	0.8	6
116	Pulsed laser deposition of hard and superhard carbon thin films from C60 targets. Diamond and Related Materials, 2010, 19, 7-14.	1.8	26
117	Superhard Properties of Rhodium and Iridium Boride Films. ACS Applied Materials & Interfaces, 2010, 2, 581-587.	4.0	60
118	Anomalous Hardening Behavior of a Calcium Phosphate Bone Cement. Journal of Physical Chemistry B, 2010, 114, 973-979.	1.2	18
119	In Situ Time-Resolved Studies of Octacalcium Phosphate and Dicalcium Phosphate Dihydrate in Simulated Body Fluid: Cooperative Interactions and Nanoapatite Crystal Growth. Crystal Growth and Design, 2010, 10, 3824-3834.	1.4	25
120	In situ time-resolved X-ray diffraction study of evolution of nanohydroxyapatite particles in physiological solution. Materials Science and Engineering C, 2009, 29, 1140-1143.	3.8	5
121	Deposition and characterization of superhard biphasic ruthenium boride films. Acta Materialia, 2009, 57, 673-681.	3.8	40
122	Physicochemical Investigation of Pulsed Laser Deposited Carbonated Hydroxyapatite Films on Titanium. ACS Applied Materials & Interfaces, 2009, 1, 1813-1820.	4.0	47
123	New Hard and Superhard Materials: RhB _{1.1} and IrB _{1.35} . Chemistry of Materials, 2009, 21, 1407-1409.	3.2	61
124	Electron beam deposited VC and NbC thin films on titanium: Hardness and energy-dispersive X-ray diffraction study. Surface and Coatings Technology, 2008, 202, 2162-2168.	2.2	21
125	Atomic fluorine in cobalt trifluoride thermolysis. Journal of Fluorine Chemistry, 2008, 129, 529-534.	0.9	2
126	Energy dispersive X-ray diffraction study of phase development during hardening of calcium phosphate bone cements with addition of chitosan. Acta Biomaterialia, 2008, 4, 1089-1094.	4.1	27

#	Article	IF	CITATIONS
127	Pulsed laser deposited hard TiC, ZrC, HfC and TaC films on titanium: Hardness and an energy-dispersive X-ray diffraction study. Surface and Coatings Technology, 2008, 202, 1455-1461.	2.2	61
128	Stabilization of Carbonate Hydroxyapatite by Isomorphic Substitutions of Sodium for Calcium. Russian Journal of Inorganic Chemistry, 2008, 53, 164-168.	0.3	20
129	Hardness of zirconium diboride films deposited on titanium substrates. Materials Chemistry and Physics, 2008, 112, 504-509.	2.0	18
130	Phase development in the hardening process of two calcium phosphate bone cements: an energy dispersive X-ray diffraction study. Materials Research Bulletin, 2008, 43, 561-571.	2.7	24
131	Superhard Rhenium Diboride Films: Preparation and Characterization. Chemistry of Materials, 2008, 20, 4507-4511.	3.2	68
132	Thermal stability and related thermodynamic properties of N-ethylthiourea. Thermochimica Acta, 2007, 460, 50-52.	1.2	3
133	Vickers and Knoop hardness of electron beam deposited ZrC and HfC thin films on titanium. Surface and Coatings Technology, 2006, 200, 4701-4707.	2.2	34
134	Carbonate release from carbonated hydroxyapatite in the wide temperature rage. Journal of Materials Science: Materials in Medicine, 2006, 17, 597-604.	1.7	78
135	Carbonate loss from two magnesium-substituted carbonated apatites prepared by different synthesis techniques. Materials Research Bulletin, 2006, 41, 485-494.	2.7	17
136	Investigation of reactions between [60]fullerene and molecular fluorine in a CoF2 matrix. Journal of Fluorine Chemistry, 2005, 126, 785-790.	0.9	5
137	Formation of the negative cluster ions in a Knudsen cell at low temperatures. International Journal of Mass Spectrometry, 2005, 245, 90-93.	0.7	8
138	Raman and infrared spectroscopic study of C60F18, C60F36 and C60F48. Vibrational Spectroscopy, 2004, 34, 137-147.	1.2	17
139	Hardness of electron beam deposited titanium carbide films on titanium substrate. Journal of Materials Science, 2004, 39, 329-330.	1.7	20
140	FTIR study of carbonate loss from carbonated apatites in the wide temperature range. Journal of Biomedical Materials Research Part B, 2004, 71B, 441-447.	3.0	45
141	In situ Very-High-Energy Diffraction Studies of Thermal Decomposition of Transition Metal Trifluorides ChemInform, 2003, 34, no.	0.1	0
142	Mass spectrometric and FTIR spectroscopic identification of FeF4 molecules in gaseous phase. Inorganic Chemistry Communication, 2003, 6, 643-645.	1.8	14
143	In Situ Very-High-Energy Diffraction Studies of Thermal Decomposition of Transition Metal Trifluorides. Bulletin of the Chemical Society of Japan, 2003, 76, 1165-1169.	2.0	3
144	Observation of a New Co-F Compound Detected by Very-High-Energy X-ray Diffraction During Thermal Decomposition of CoF3. Chemistry Letters, 2002, 31, 664-665.	0.7	1

#	Article	IF	CITATIONS
145	Mass spectrometric determination of the dissociation energy of Mn2F6(g). Rapid Communications in Mass Spectrometry, 2002, 16, 1526-1530.	0.7	2
146	Selective formation of C60F18(g) and C60F36(g) by reaction of [60]fullerene with molecular fluorine. Journal of Fluorine Chemistry, 2002, 113, 219-226.	0.9	14
147	Mass and FTIR Spectroscopic Investigations of Gaseous Manganese Tetrafluoride. Inorganic Chemistry, 2001, 40, 179-181.	1.9	11
148	Transition and rare earth metal fluorides as thermal sources of atomic and molecular fluorine. European Physical Journal Special Topics, 2001, 11, Pr3-109-Pr3-113.	0.2	3
149	In situ time-resolved X-ray diffraction study of manganese trifluoride thermal decomposition. Journal of Fluorine Chemistry, 2001, 108, 253-256.	0.9	9
150	Sublimation properties of CoF3: mass spectrometric and quantum chemical studies. Rapid Communications in Mass Spectrometry, 2001, 15, 749-757.	0.7	7
151	Mass spectrometric determination of appearance energies for ions formed from CoF4 and CoF3 molecules. , 2000, 14, 459-463.		2
152	Atomic fluorine in thermal reactions involving solid TbF4. Journal of Fluorine Chemistry, 2000, 104, 291-295.	0.9	25
153	Identification of Gaseous Cobalt Tetrafluoride:  MS and FTIR Spectroscopic Studies. Inorganic Chemistry, 1999, 38, 5695-5697.	1.9	18
154	Mass Spectrometry Study of C60and C60-NiF2Fluorination with Molecular Fluorine. Fullerenes, Nanotubes, and Carbon Nanostructures, 1998, 6, 577-598.	0.6	11
155	Mass spectrometric determination of cobalt trifluoride saturated vapor pressure. Enthalpy of formation of gaseous CoF4 and CoF4â^. Rapid Communications in Mass Spectrometry, 1997, 11, 1977-1979.	0.7	7
156	<i>In Situ</i> Time-Resolved Energy Dispersive X-Ray Diffraction Studies of Calcium Phosphate Based Bone Cements. Key Engineering Materials, 0, 541, 115-120.	0.4	5